Quark Matter, Wuhan, 06.11.19

# Skewness and kurtosis of net strangeness, net baryon-number and net electric-charge distributions at non-zero $\mu_B$

F. Karsch[1], S. Mukherjee[2], C. Schmidt[1] and D. Bollweg[1]
HotQCD Collaboration

[1]Bielefeld University [2]Brookhaven National Lab

# Outline

# QCD Phase Diagram

- Smooth crossover for $\mu_B < 300$ MeV.
- Recent result from lattice QCD [arXiv:1812.08235]:

$$T_{pc}(\mu_B) = T_{pc,0}\left(1 - \kappa_2^{B,f}\bar{\mu}_B^2 - \kappa_4^{B,f}\bar{\mu}_B^4\right)$$

$$\text{with } \bar{\mu}_B = \frac{\mu_B}{T_{pc,0}},\ T_{pc,0} = 156.5 \pm 1.5\ \mathrm{MeV},$$

$$\kappa_2^{B,f} = 0.012 \pm 0.004,$$

$$\kappa_4^{B,f} = 0.000 \pm 0.004$$

- Rest of the phase diagram largely unknown.

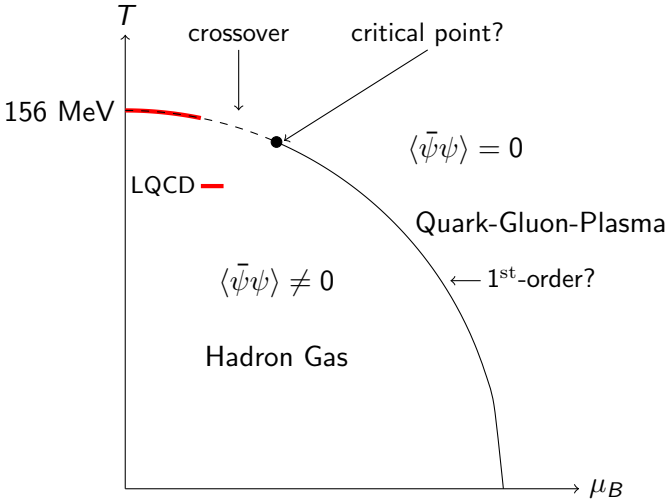

# QCD Phase Diagram

- Chiral crossover overlaps with chemical freeze-out in heavy ion collisions: $T_{cf}(\mu_B \sim 0) = 156.5$ MeV [Andronic et al. Nature 2018].
- Transition region is accessible through HIC experiments.
- Cumulants of conserved charge fluctuations are ideal probes to study phase diagram: maxima along crossover line, divergence at CEP.
- Experiments: STAR at RHIC and ALICE at LHC.

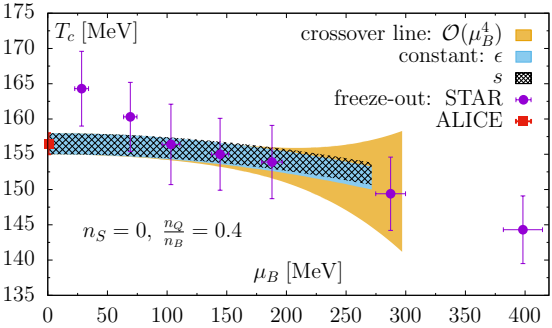


Figure 1: Freeze-out vs. chiral transition temperature from HotQCD [arXiv:1812.08235].

**Goal: first-principle QCD predictions for cumulant ratios $M/\sigma^2, S\sigma, \kappa\sigma^2, \ldots$ etc.**

# Fluctuations via lattice QCD

$M/\sigma^2, S\sigma, \kappa\sigma^2$ are accessible via *generalized susceptibilities* $\chi$:

$$\chi_{ijk}^{BQS} \equiv \frac{1}{TV^3} \frac{\partial^{i+j+k} \log \mathcal{Z}}{\partial \hat{\mu}_B^i \partial \hat{\mu}_Q^j \partial \hat{\mu}_S^k}, \quad \hat{\mu}_X \equiv \frac{\mu_X}{T}$$

$$M_X/\sigma_X^2 = \frac{\chi_1^X}{\chi_2^X}, S_X\sigma_X = \frac{\chi_3^X}{\chi_2^X}, \kappa_X\sigma_X^2 = \frac{\chi_4^X}{\chi_2^X} \text{ with } X = B, Q, S$$

- Finite-density sign problem renders direct simulations at $\mu_B > 0$ impossible.
- Use constrained Tayor-Expansion in $\mu$ to access cumulants at finite density.
- Impose strangeness neutrality $n_S = 0$ and $\frac{n_Q}{n_B} = 0.4$ order by order - corresponds to thermal conditions in HIC (e.g. Pb + Pb or Au + Au).
- Computationally demanding: At $\mathcal{O}(N)$ we need to calculate ALL $\chi_{ijk}^{BQS}$ with $i + j + k \leq N$ at $\mu_B = 0$.

# Fluctuations via lattice QCD - Setup

- Dynamical Fermions (HISQ) with $N_f = 2 + 1$: two light Quarks (up + down) and a strange Quark with mass ratio $\frac{m_s}{m_l} = 27$. $\Rightarrow$ physical meson masses in the continuum limit!
- Lattice sizes $32^3 \times 8$, $48^3 \times 12$ and $64^3 \times 16$ at 9 different temperatures each.
- Large simulation campaign on Summit in 2019: Compared to our earlier analysis of skewness and kurtosis [arXiv:1708.04897v3] we increased statistics in the vicinity of $T_{pc}$ on $N_t = 8$ lattices by a factor 3-4 and on $N_t = 12$ lattices by a factor 6-8.

| | $N_t = 8$ | $N_t = 12$ | $N_t = 16$ |
|---|---|---|---|
| No. of Conf. | $1.2 \cdot 10^6$ | $2 - 3 \cdot 10^5$ | $10^4$ |

- High statistics data enable us to calculate cumulants up to $\mathrm{N^3LO}$ in $\mu_B$ (previous studies: $\mathrm{NLO}$).


Summit: $\sim$ 4600 compute nodes: 1 node = 6 V100 GPUs and 2 CPUs

# Fluctuations via lattice QCD - towards $R_{nm}(T_{\rm pc}(\mu_B))$

- Cumulant ratios are scanned in $\mu_B$

$$R^X_{nm}(T,\mu_B) = \frac{\sum_i \frac{1}{i!}\chi^{X,i}_n(\frac{\mu_B}{T})^i}{\sum_j \frac{1}{j!}\chi^{X,j}_m(\frac{\mu_B}{T})^j}$$

- Results like Fig. 2 for each $N_t$ are jointly fitted assuming $1/N_t^2$ corrections $\rightarrow$ continuum extrapolation.
- The fitted surface can then be evaluated along arbitrary lines in $(T,\mu_B)$ if desired. In the following: $T_{\rm pc}(\mu_B)$

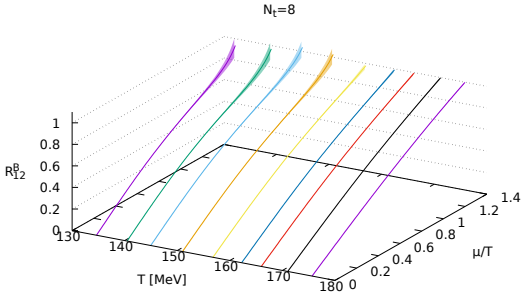


Figure 2: $R^B_{12}$ for $N_t = 8$ scanned in $\mu_B/T$.

# Results - $R_{12}^B$

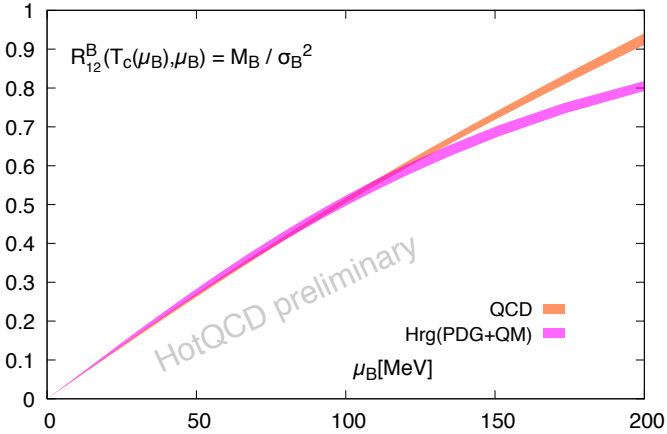


Figure 3: Continuum extrapolation of $R_{12}^B(T_{\rm pc}(\mu_B))$ vs HRG.

- Agreement with HRG up to $\mu_B \sim 120$ MeV.
- $R_{12}^B$ can be used to eliminate $\mu_B$ in higher order cumulant ratios.

# Results - $R_{12}^B$

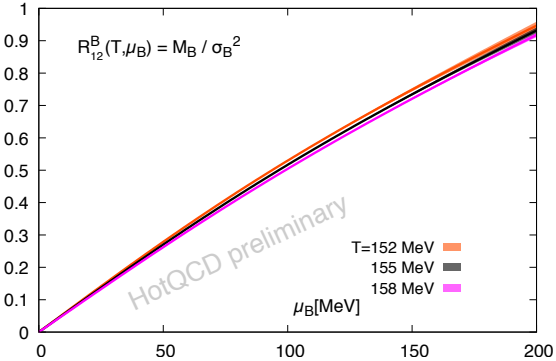


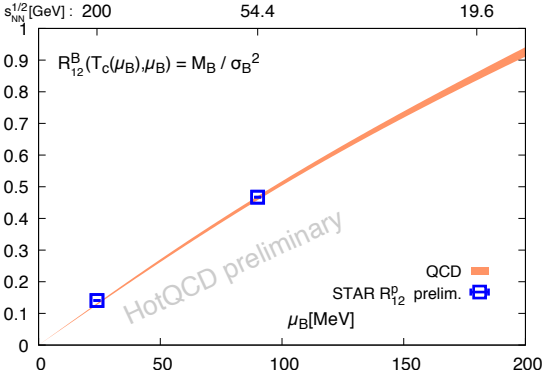


Figure 4: $T$-variation of $R_{12}^B$ and $R_{12}^B$ vs prelim. STAR results.

# Results - $R^B_{31}$ and $R^B_{42}$

Reminder: $155\ \mathrm{MeV} < T_{pc} < 158\ \mathrm{MeV}$

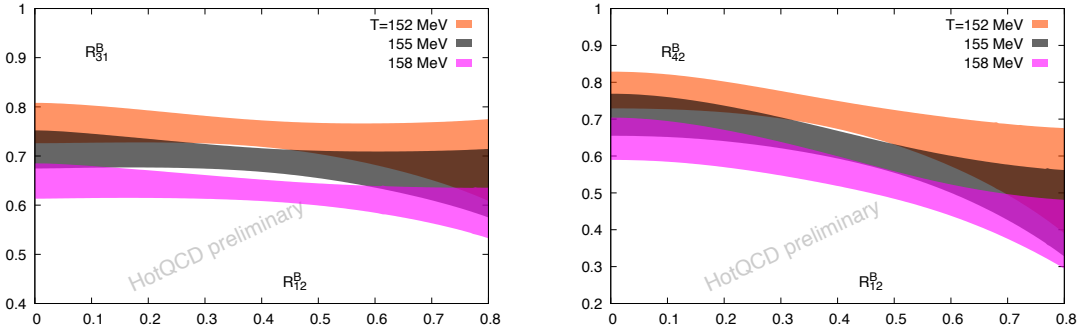


Figure 5: Continuum estimates of $R^B_{31}(R^B_{12})$ and $R^B_{42}(R^B_{12})$ at various $T$.

# Results - $R^B_{31}$ and $R^B_{42}$

- STAR data at $\sqrt{s} = 54.4$ GeV favors freeze-out slightly below $T_{\rm pc}$.
- STAR result $T_f \sim 165$ MeV at $\sqrt{s} = 200$ GeV is not consistent with determination of freeze-out temperature from measured cumulant ratios.

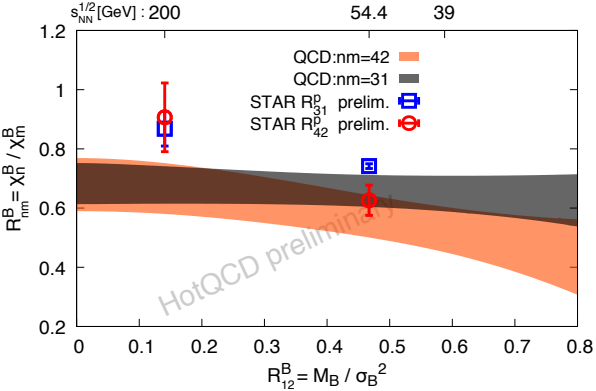


Figure 6: Continuum estimates of $R^B_{31}(R^B_{12})$ and $R^B_{42}(R^B_{12})$ vs prelim. STAR results.

# Results - $R^B_{51}$ & $R^B_{62}$

- High statistics enables us to estimate $R^B_{62}$ at NLO in $\mu_B$.
- A. Pandav @SQM2019: $R^p_{62}(\sqrt{s} = 200\ \mathrm{GeV}) < 0$, $R^p_{62}(\sqrt{s} = 54.4\ GeV) > 0$
- Lattice QCD estimate:

| $\sqrt{s}$ | $R^B_{51}$ | $R^B_{62}$ |
|---|---|---|
| 200 GeV | -0.5(3) | -0.7(3) |
| 54.4 GeV | -0.7(4) | -2(1) |

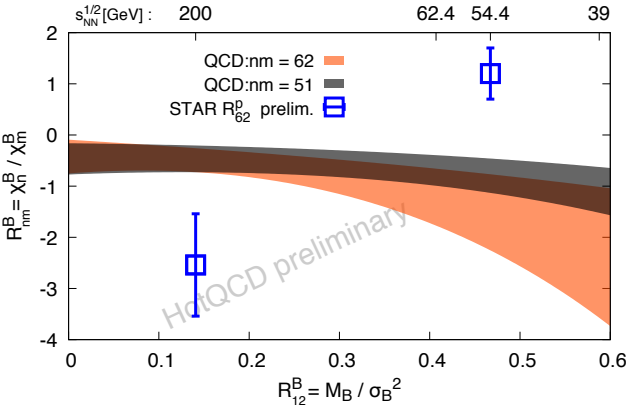


Figure 7: $R^B_{51}$ and $R^B_{62}$ at NLO for $N_t = 8$ lattices vs prelim. STAR results.

# Teaser - Charge Fluctuations

"Baryometer" & "Thermometer"

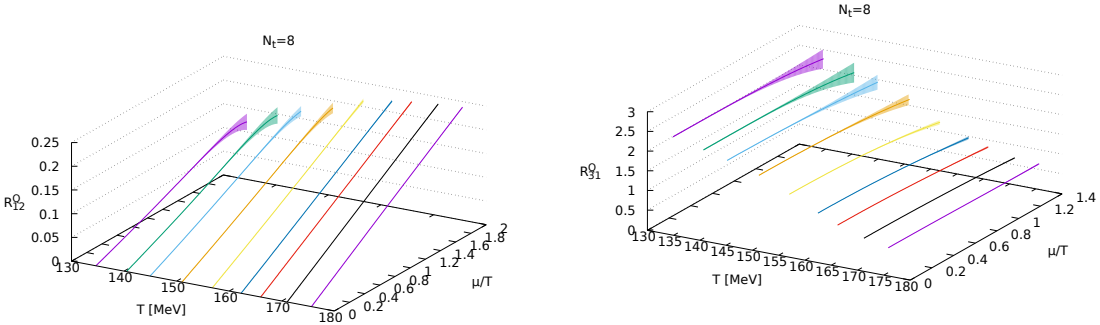


Figure 8: $R^Q_{12}$ and $R^Q_{31}$ in the $(T, \mu_B/T)$ plane.

# Summary & Outlook

- So far:
- Significantly increased precision compared to previous studies: $M/\sigma^2$ up to $N^3LO$ in $\mu_B$.
- First estimations of $R_{51}^B$ and $R_{62}^B$ are now possible.
- Not shown here: various correlations like $\chi_{1n}^{BQ}$ and $\chi_{1n}^{BS}$ up to $n = 7$.
- In the future:
- Increased focus on $N_t = 12$ and $N_t = 16$ in 2020 using new Multi-GPU Code.